Science Advances
AAAS

Supplementary Materials for

SMAD4, activated by the TCR-triggered MEK/ERK signaling pathway, critically regulates $CD8^+$ T cell cytotoxic function

Xinwei Liu *et al.*

Corresponding author: Chen Dong, chendong@tsinghua.edu.cn

Sci. Adv. **8**, eabo4577 (2022)
DOI: 10.1126/sciadv.abo4577

The PDF file includes:

Figs. S1 to S9
Legends for supplemental excel files S1 to S3

Other Supplementary Material for this manuscript includes the following:

Supplemental excel files S1 to S3

Figure S1

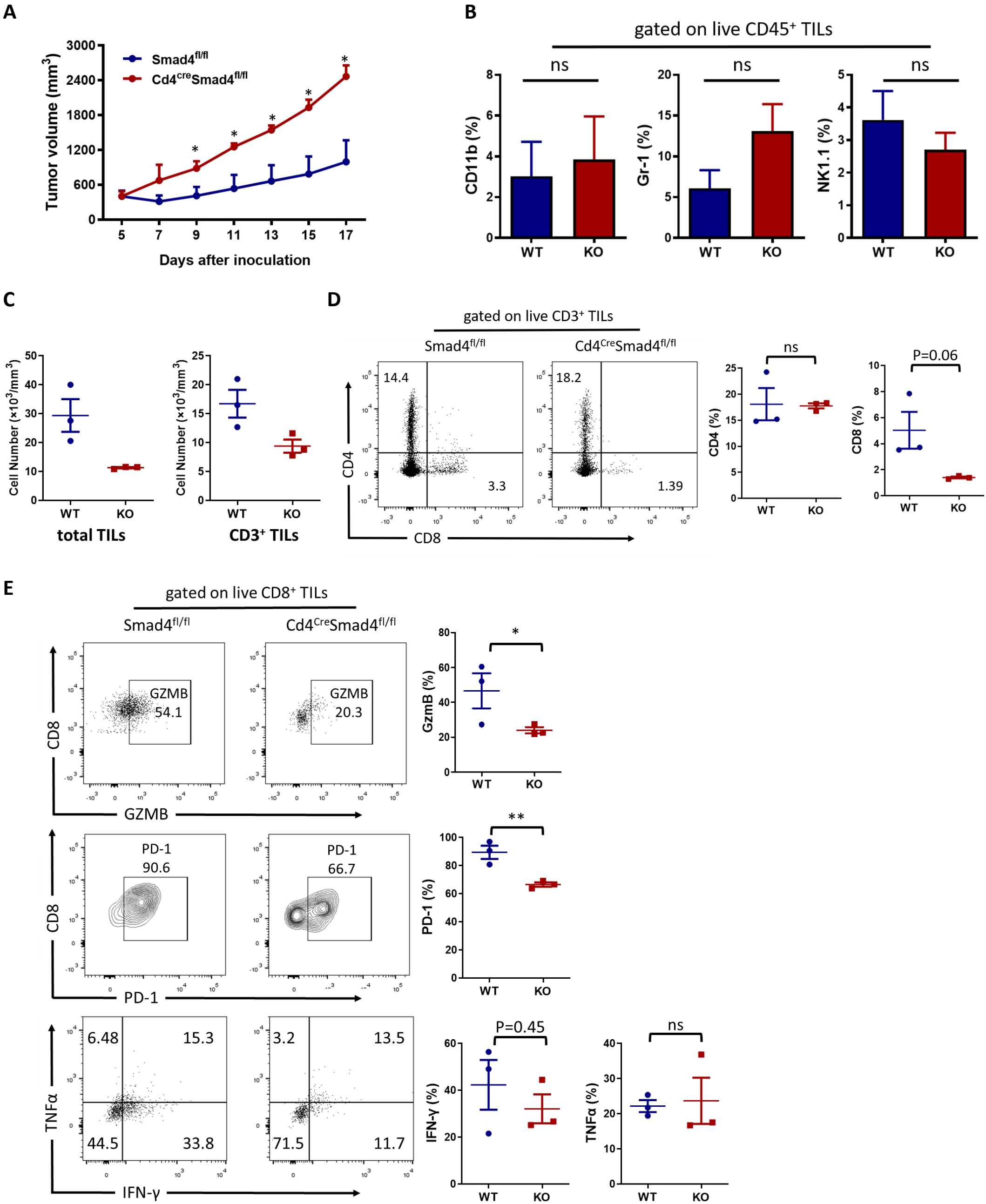
A
Smad4fl/fl
Cd4creSmad4fl/fl
Tumor volume (mm3)
Days after inoculation
B
gated on live CD45+ TILs
ns
CD11b (%)
Gr-1 (%)
NK1.1 (%)
WT
KO
C
Cell Number (×10³/mm³)
total TILs
CD3+ TILs
D
gated on live CD3+ TILs
Smad4fl/fl
Cd4CreSmad4fl/fl
14.4
3.3
18.2
1.39
CD4
CD8
CD4 (%)
CD8 (%)
P=0.06
E
gated on live CD8+ TILs
GZMB
54.1
20.3
GzmB (%)
*
PD-1
90.6
66.7
PD-1 (%)
**
6.48
15.3
44.5
33.8
3.2
13.5
71.5
11.7
TNFα
IFN-γ
IFN-γ (%)
P=0.45
TNFα (%)

Figure S1

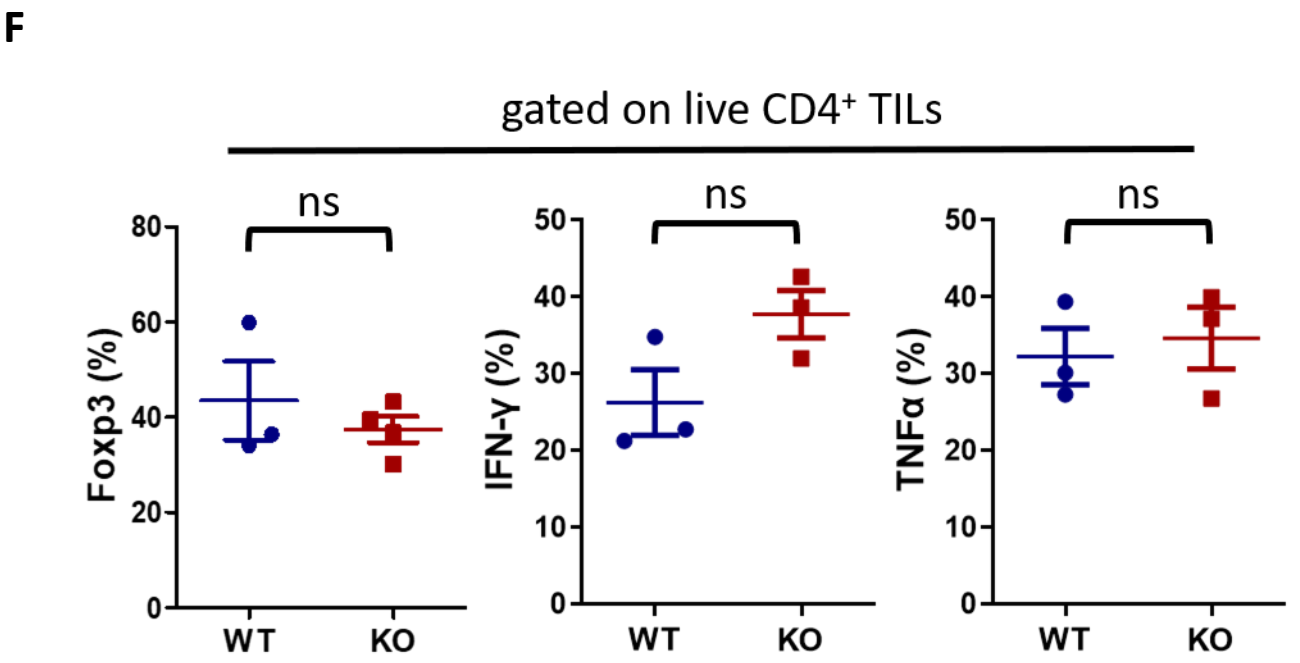

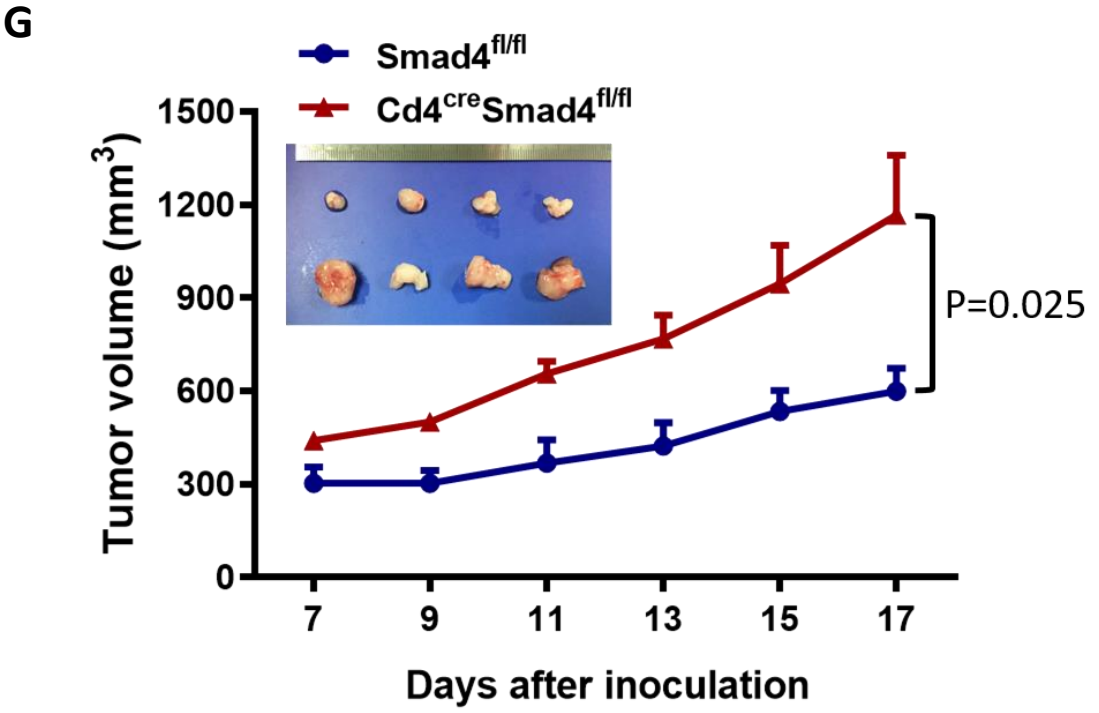

Figure S1 SMAD4 deficiency in T lymphocytes promoted cancer progression.
(A) E.G7 cells (1×10^6 cells per mouse) were inoculated subcutaneously into wild-type (n=5) or *Cd4*^{Cre}*Smad4*$^{fl/fl}$ mice (n=5). Tumor growth was monitored from day 5 after inoculation. (B) Expression levels of CD11b, Gr-1 and NK1.1 among CD45$^+$ TILs from E.G7 tumor bearing WT and *Cd4*^{Cre}*Smad4*$^{fl/fl}$ mice. (C) Tumor infiltrating lymphocytes were isolated at day 17 from E.G7 tumor bearing mice. Total TILs numbers per mm^3 were calculated by hemocytometer, CD3$^+$ TILs number was calculated by flow cytometry. (D) Representative figures and summary data showing surface expression of CD4 and CD8 in CD3$^+$ TILs from E.G7 tumor bearing WT and *Cd4*^{Cre}*Smad4*$^{fl/fl}$ mice. Measured by flow cytometry. (E) Expression levels of PD-1 in CD8$^+$ TILs and production of Granzyme B, TNFα and IFN-γ after PMA and ionomycin stimulation in CD8$^+$ TILs from E.G7 tumor bearing WT and *Cd4*^{Cre}*Smad4*$^{fl/fl}$ mice. (F) Expression levels of Foxp3, TNFα and IFN-γ after PMA and ionomycin stimulation in CD4$^+$ TILs from E.G7 tumor bearing WT and and *Cd4*^{Cre}*Smad4*$^{fl/fl}$ mice. (G) MC38 cells (1×10^6 cells per mouse) were inoculated subcutaneously into wild-type (n=4) or *Cd4*^{Cre}*Smad4*$^{fl/fl}$ mice (n=4). Tumor growth were monitored from Day 7 after inoculation. These experiments were repeated three times. Data are represented as mean ± SEM. n.s., not significant. *p < 0.05, **p < 0.01.

Figure S2

A

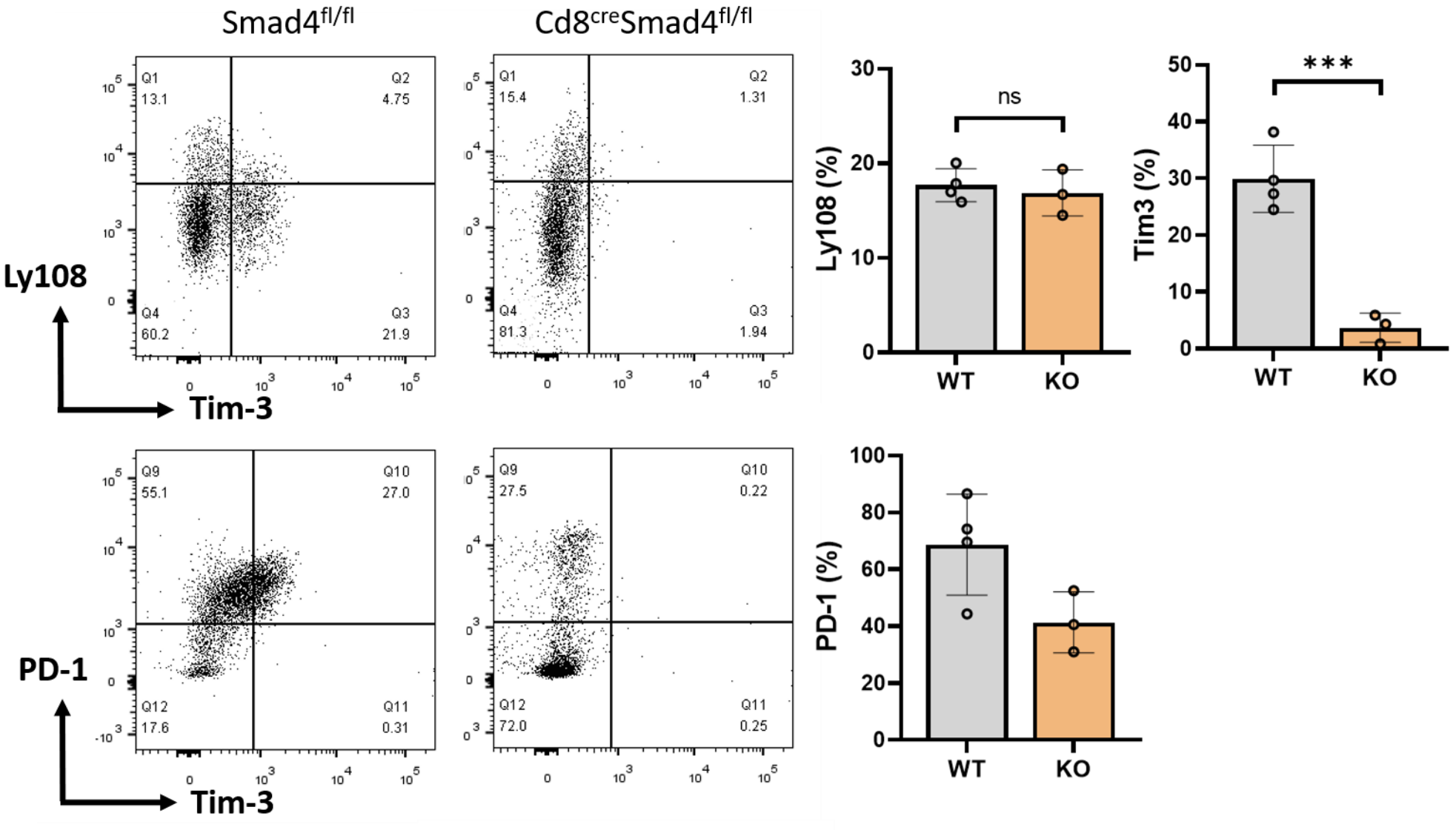
Smad4fl/fl
Cd8creSmad4fl/fl
Ly108
Tim-3
Q1 13.1
Q2 4.75
Q4 60.2
Q3 21.9
Q1 15.4
Q2 1.31
Q4 81.3
Q3 1.94
Ly108 (%)
ns
WT
KO
Tim3 (%)
***
PD-1
Q9 55.1
Q10 27.0
Q12 17.6
Q11 0.31
Q9 27.5
Q10 0.22
Q12 72.0
Q11 0.25
PD-1 (%)

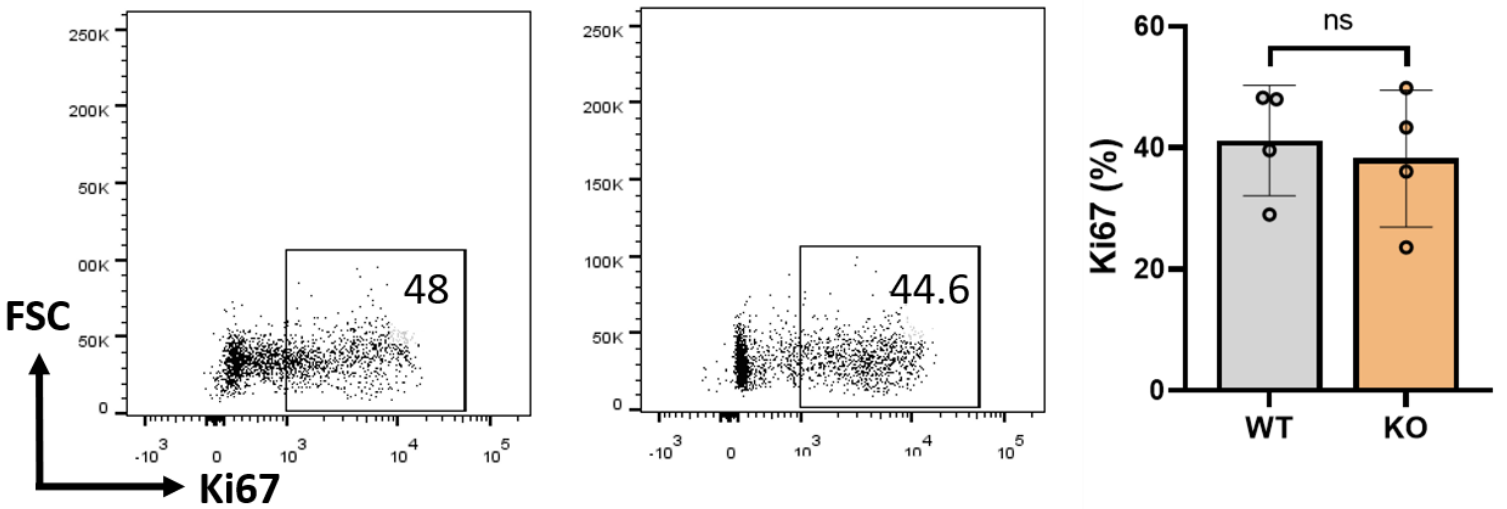
FSC
Ki67
48
44.6
Ki67 (%)
ns
WT
KO

Figure S2

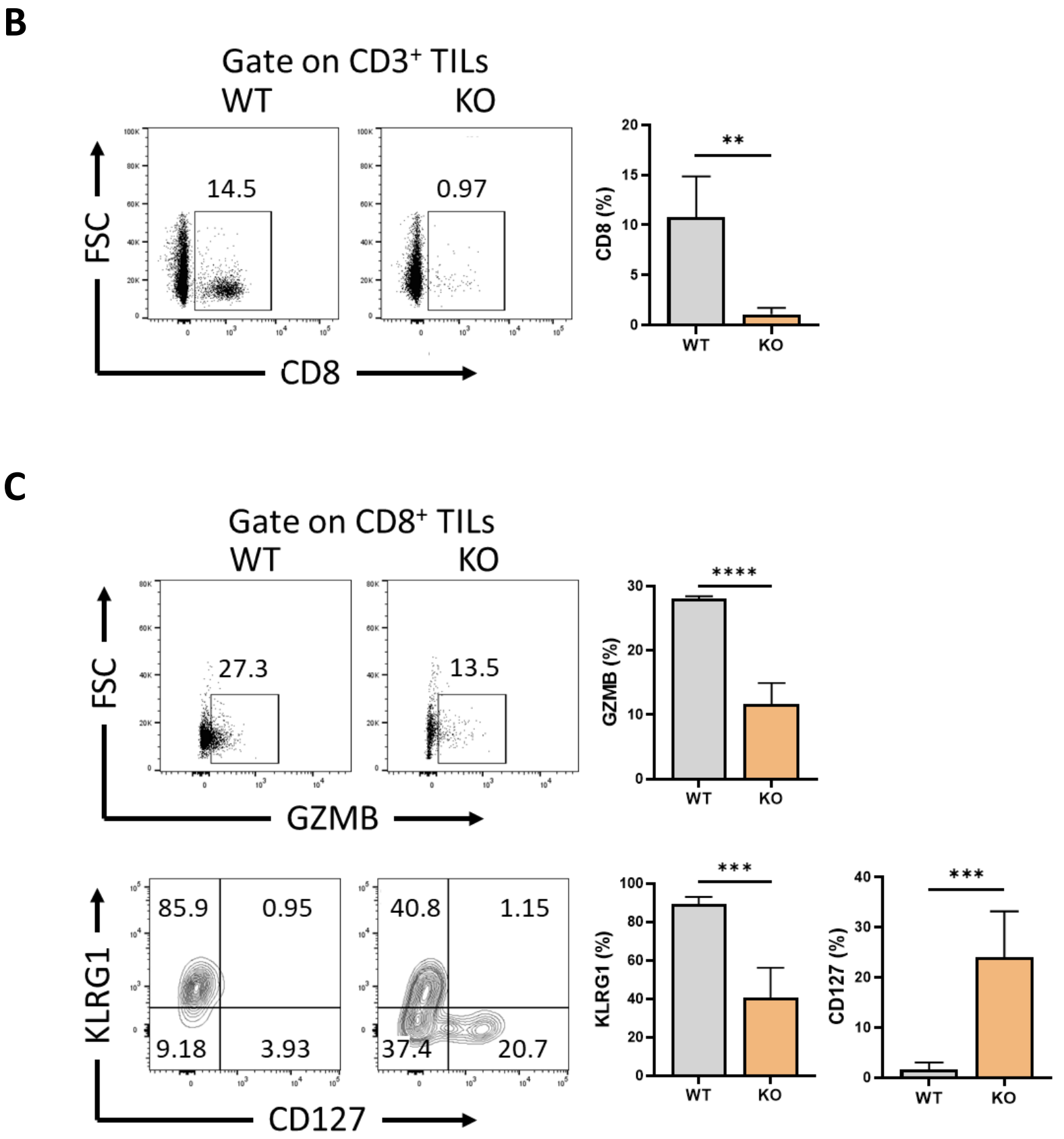

Figure S2 Expression levels of PD-1, TIM-3, Ly108 and Ki-67 in CD8$^+$ TILs from E.G7 tumor bearing WT and *Cd8*^{Cre}*Smad4*$^{fl/fl}$ mice.

(A) Expression levels of PD-1, TIM-3, Ly108 and Ki-67 in CD8$^+$ TILs from E.G7 tumor bearing WT and Cd8^{Cre}Smad4$^{fl/fl}$ mice. **(B-C)** TILs were isolated at day 17 from E.G7-bearing mice and re-stimulated by $OVA_{257-264}$-peptide (10 ng/ml). Then CD8 proportion and the expression levels of GZMB, CD127 and KLRG1 were measured by flow cytometry. Data are represented as mean ± SEM. The statistics were performed by Student's t test. n.s., not significant. **p < 0.01, ***p < 0.001, ****p < 0.0001.

Figure S3

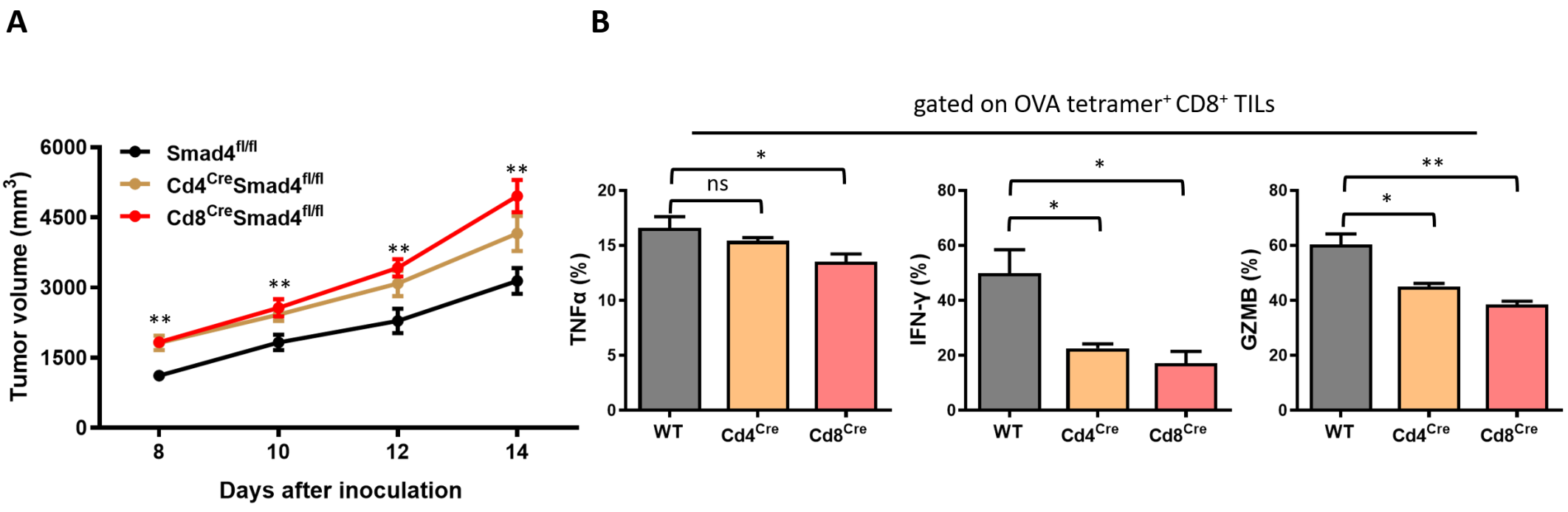

Figure S3 E.G7 tumor growth and antigen-specific CD8⁺ T cell cytotoxic function showed no differences between *Cd8*^{Cre}*Smad4*$^{fl/fl}$ mice and *Cd4*^{Cre}*Smad4*$^{fl/fl}$ mice.

(A) E.G7 cells (1×10^6 cells per mouse) were inoculated subcutaneously into wild-type mice (n=5), *Cd4*^{Cre}*Smad4*$^{fl/fl}$ mice (n=5) and *Cd8*^{Cre}*Smad4*$^{fl/fl}$ mice (n=5). Tumor volume was monitored from Day 8 after inoculation. (B) GZMB, TNFα and IFN-γ expression in OVA-specific CD8⁺ T cells from *Cd8*^{Cre}*Smad4*$^{fl/fl}$ mice and *Cd4*^{Cre}*Smad4*$^{fl/fl}$ mice significantly reduced in contrast with WT mice. Measured by flow cytometry. Data are represented as mean ± SEM. Two-way Anova analysis. *$p < 0.05$, **$p < 0.01$.

Figure S4

A

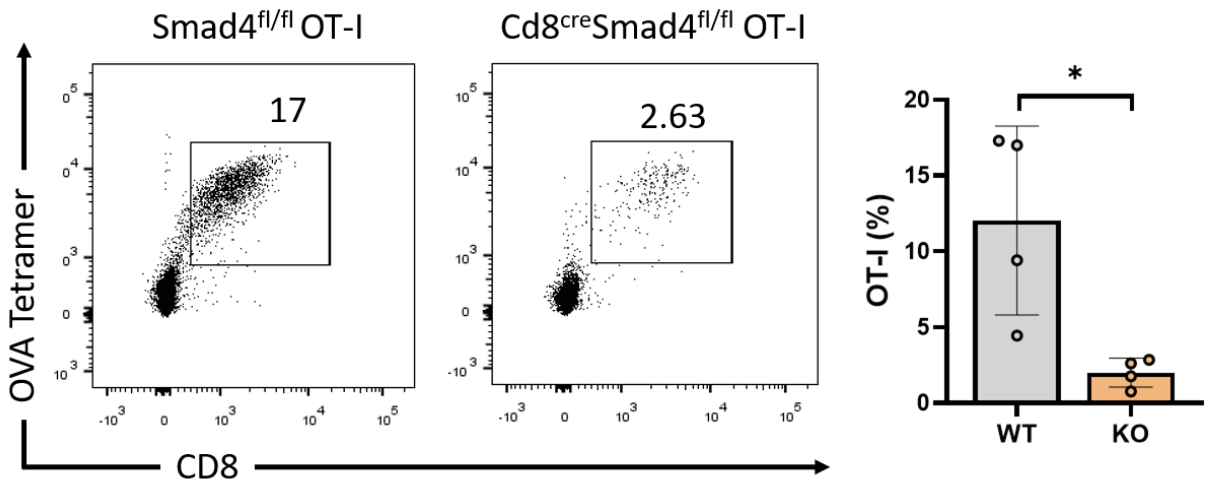

B

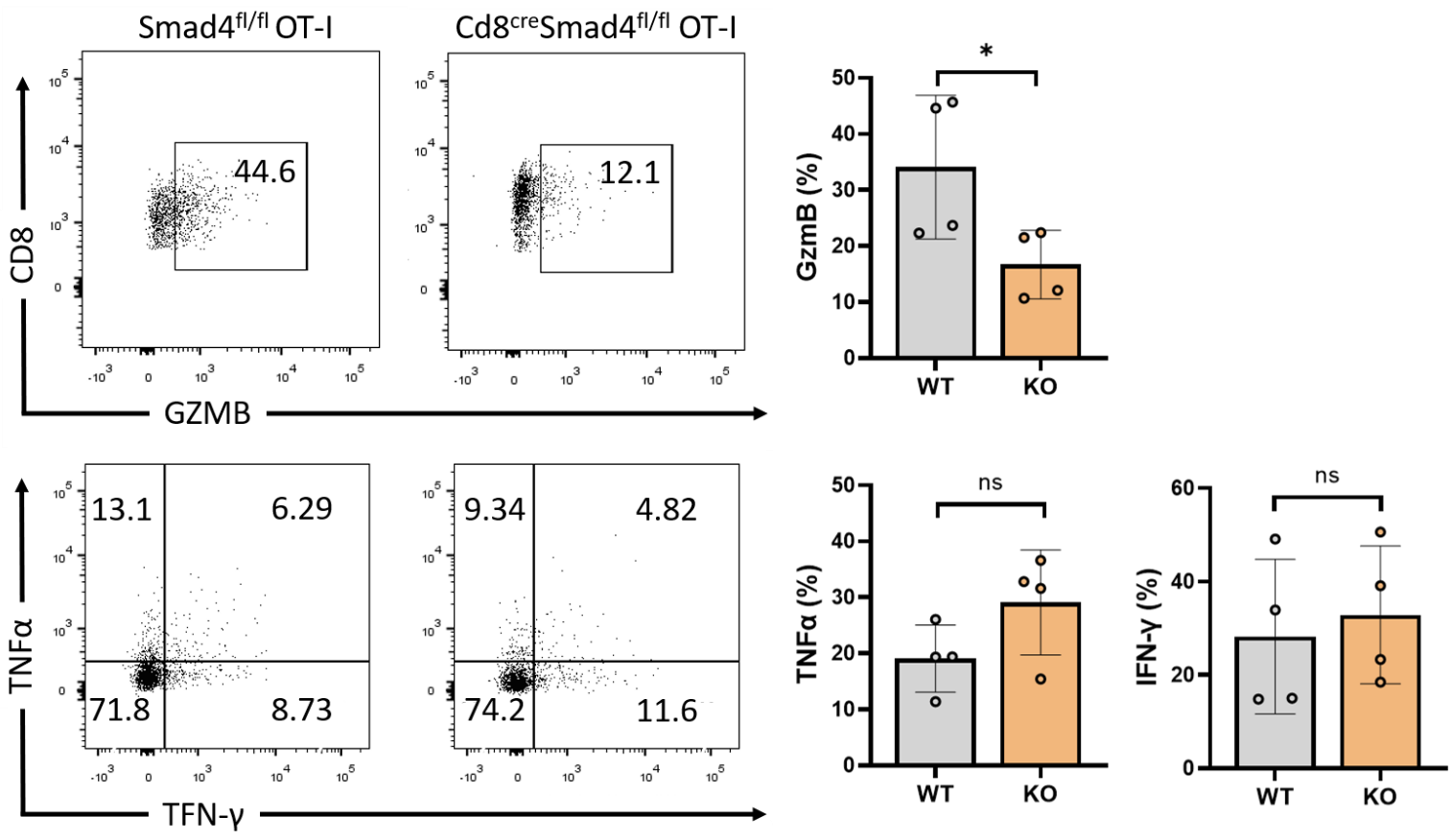

C

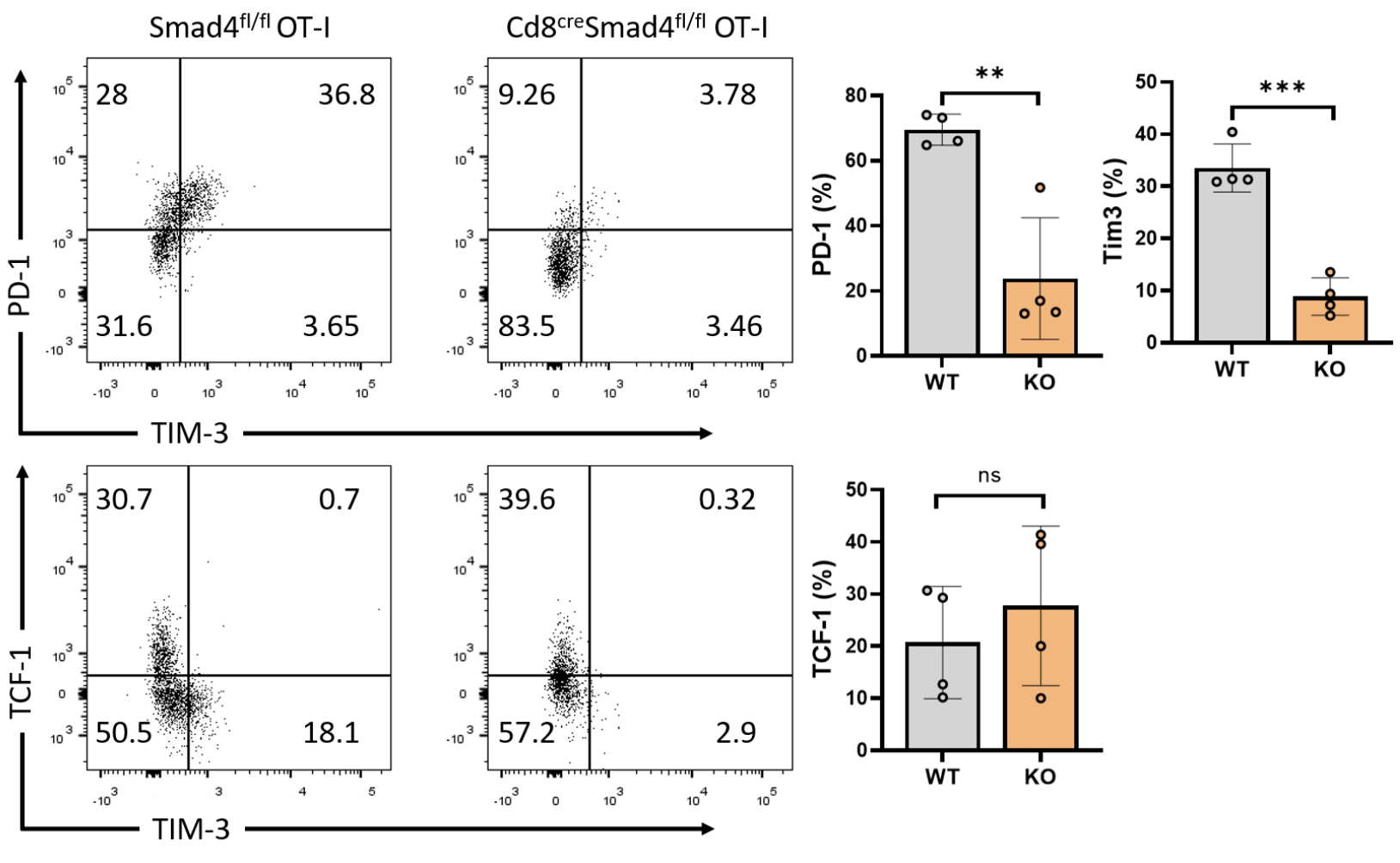

Figure S4 Flow cytometric analysis of adoptive transfer experiments.
(A) The percentage of OT-I cells in E.G7 tumor bearing *TCRbd*$^{-/-}$ mice adoptive transferring wild-type or *Smad4*$^{-/-}$ OT-I cells. (B) GZMB, TNFα and IFN-γ expression in wild-type or *Smad4*$^{-/-}$ OT-I cells. (C) TCF-1, PD-1 and TIM-3 expression in wild-type or *Smad4*$^{-/-}$ OT-I cells. Data are represented as mean ± SEM. n.s., not significant. *p < 0.05, **p < 0.01, ***p < 0.001.

Figure S5

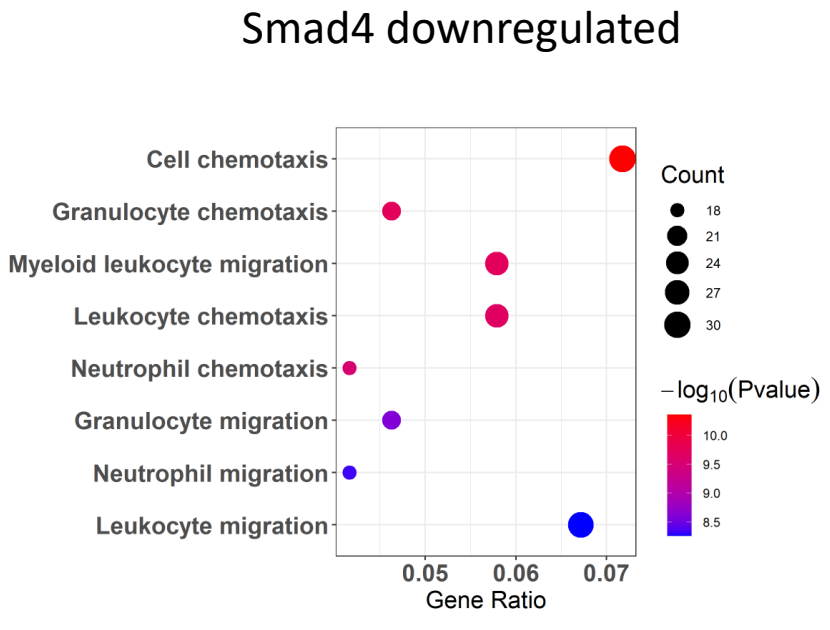

Figure S5 GO pathway analysis of SMAD4 downregulated (SMAD4-abrogation upregulated) genes. OVA-specific CD8$^+$ TILs from WT and *Cd8*^{Cre}*Smad4*$^{fl/fl}$ mice were collected and used for whole genome transcriptome analysis.

Figure S6

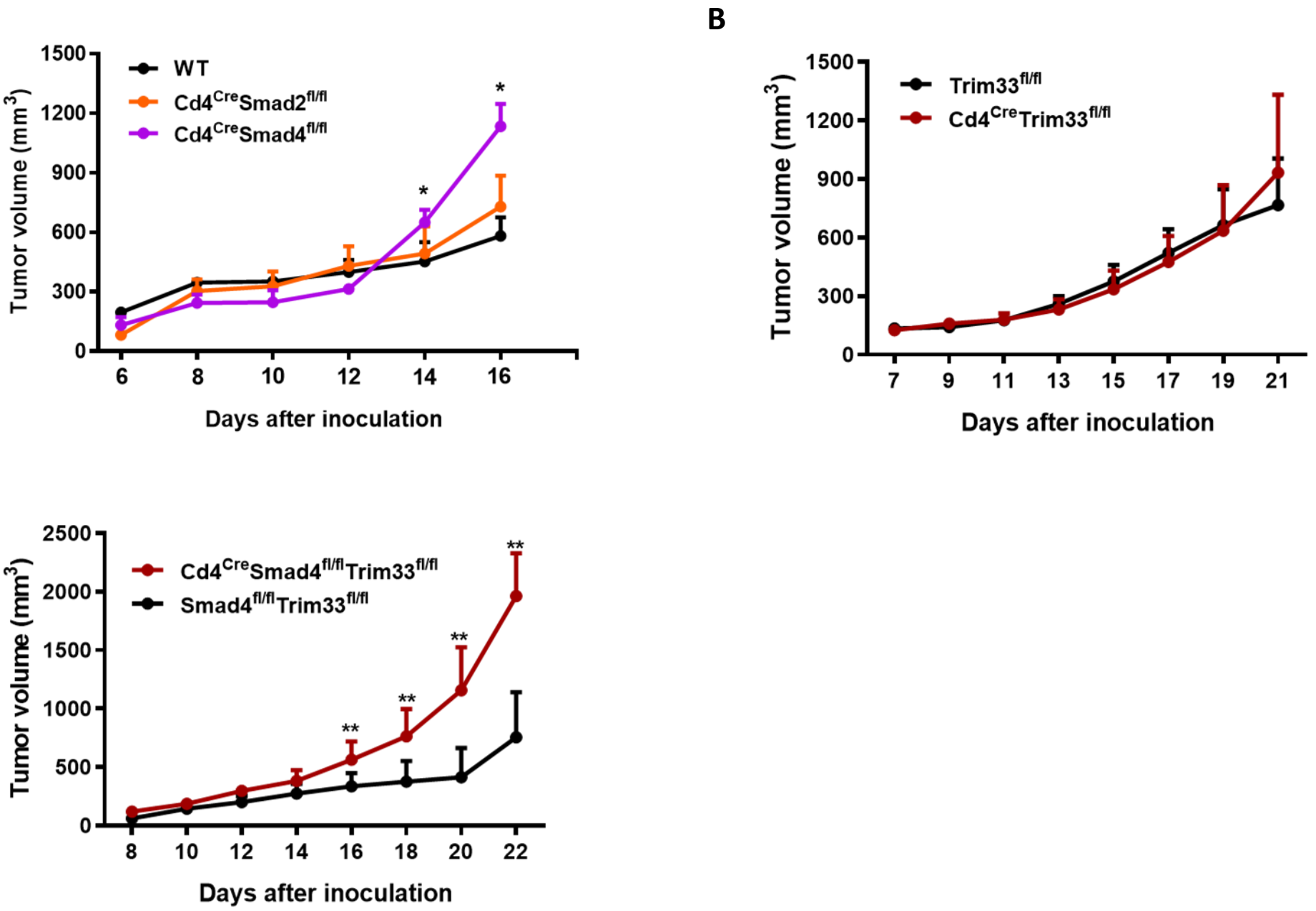

Figure S6 E.G7 tumor growth in *Cd4*^{Cre}*Smad2*$^{fl/fl}$ mice, *Cd4*^{Cre}*Trim33*$^{fl/fl}$ mice and *Cd4*^{Cre}*Smad4*$^{fl/fl}$*Trim33*$^{fl/fl}$ mice.

(A) E.G7 cells (1×10^6) were inoculated subcutaneously into wild-type mice (n=5), *Cd4*^{Cre}*Smad2*$^{fl/fl}$ mice (n=5) and *Cd4*^{Cre}*Smad4*$^{fl/fl}$ mice (n=5). Tumor growth were monitored from day 6 after inoculation. (B) E.G7 cells (1×10^6) were inoculated subcutaneously into wild-type (n=5), and *Cd4*^{Cre}*Trim33*$^{fl/fl}$ mice (n=6). Tumor growth were monitored from day 7 after inoculation. (C) E.G7 cells (1×10^6) were inoculated subcutaneously into wild-type (n=6), and *Cd4*^{Cre}*Smad4*$^{fl/fl}$*Trim33*$^{fl/fl}$ mice (n=6). Tumor growth were monitored from day 8 after inoculation. Data are represented as mean ± SEM. n.s., not significant. *$p < 0.05$, **$p < 0.01$.

Figure S7

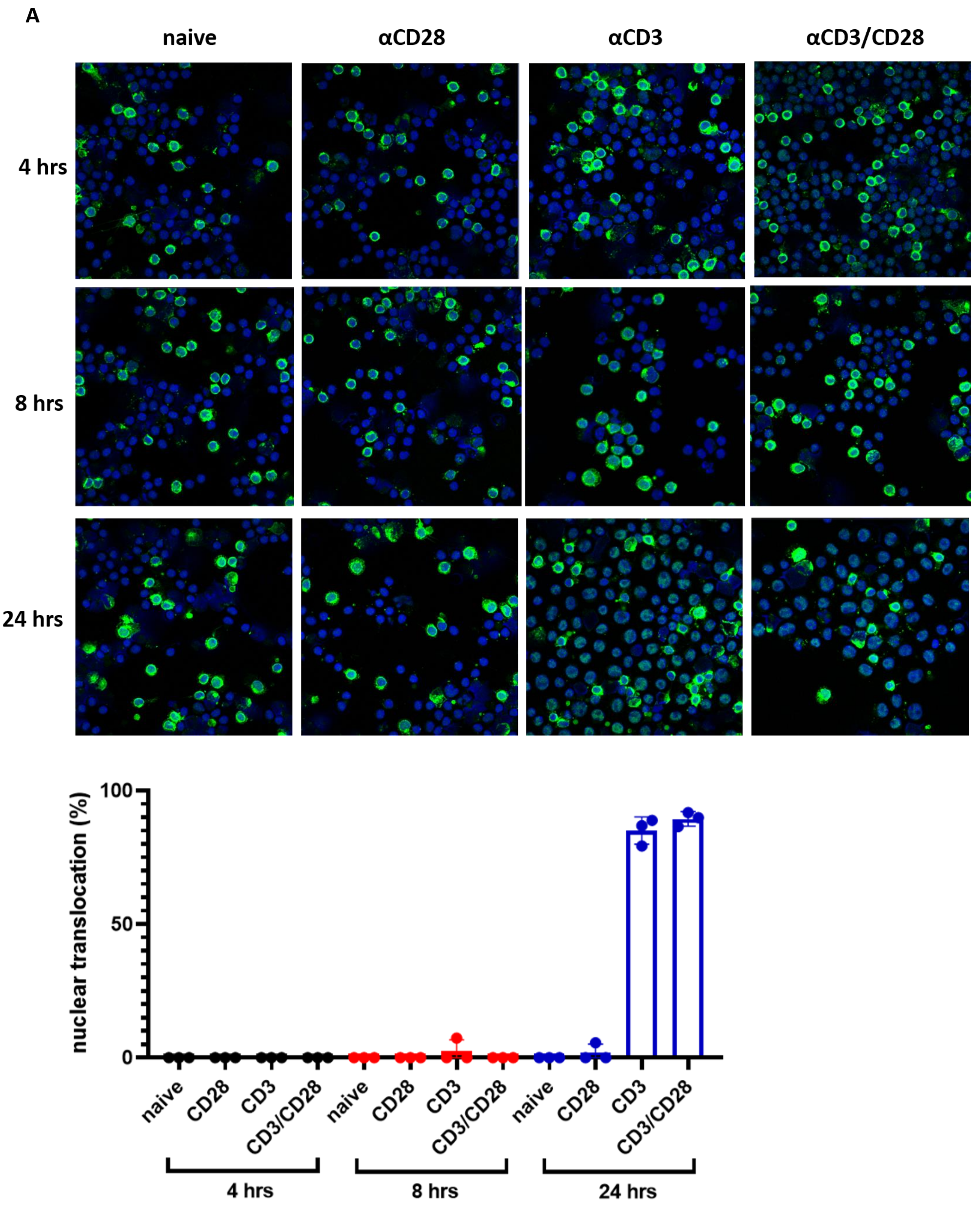
A
naive
αCD28
αCD3
αCD3/CD28
4 hrs
8 hrs
24 hrs
nuclear translocation (%)
100
50
0
naive
CD28
CD3
CD3/CD28
4 hrs
8 hrs
24 hrs

Figure S7

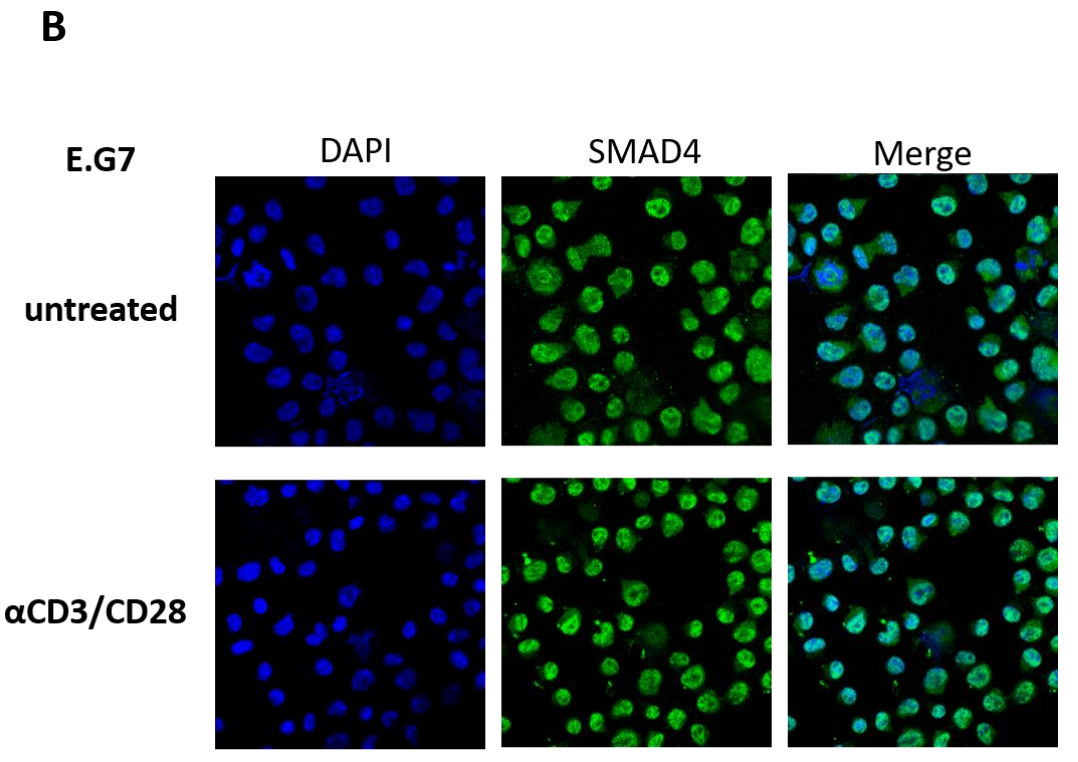

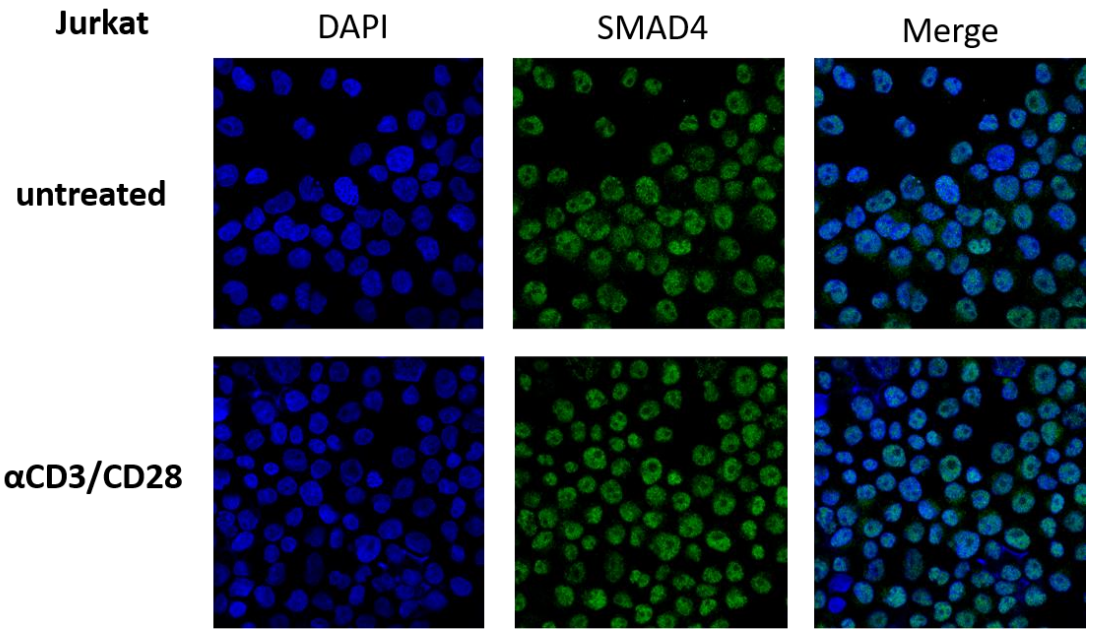

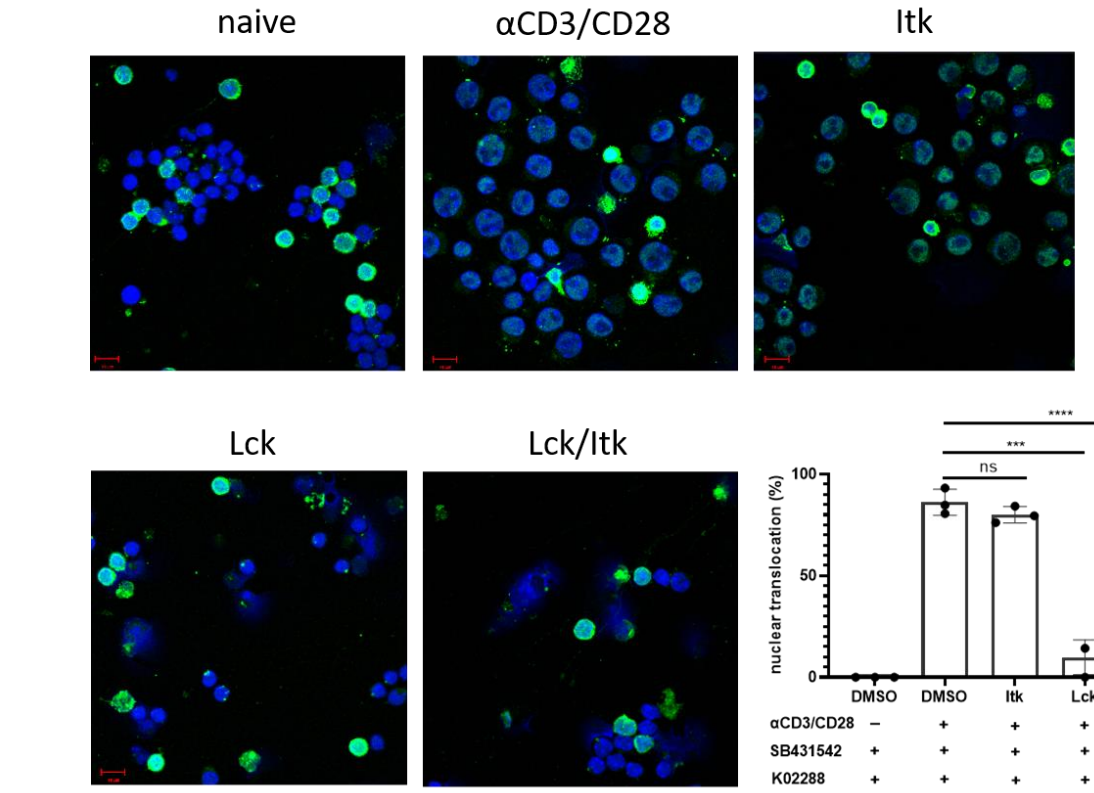

Figure S7 SMAD4 nuclear translocation in CD8$^+$ T cells is regulated by TCR activation.
(A) Subcellular localization of SMAD4 in naive and αCD3/CD28 activated CD8$^+$ T cells (activated for 4hr, 8hr, 24hr, respectively). The cells were collected, spun down to a cytospin microscope slide, and fixed and stained with αSMAD4 followed by staining with Alexa Fluor 488 conjugated secondary antibody. The results shown here represent the merged photos of SMAD4 (green) and DAPI (blue, indicated for nuclear location) staining. Down: statistic data of SMAD4 nuclear translocation ratio, which was determined by manually counting the percentage of cells containing higher SMAD4 staining intensity in the nucleus versus cytoplasm in three representative fields revealed by Image-Pro Plus software. (B) Subcellular localization of SMAD4 in E.G7 cells. Up: no αCD3/CD28 treatment. Down: αCD3/CD28 treatment. (C) Subcellular localization of SMAD4 in Jurkat cells. Up: no αCD3/CD28 treatment. Down: αCD3/CD28 treatment. (D) Subcellular localization of SMAD4 in naive and αCD3/CD28 activated CD8$^+$ T cells (in the presence of DMSO control, Itk inhibitor, Lck inhibitor and combination of Lck/Itk inhibitors, respectively). All the groups were in the presence of TGF-β receptor and BMP receptor inhibitors. The results shown here represent the merged photos of SMAD4 (green) and DAPI (blue) staining. These experiments were repeated three times. Data are represented as mean ± SEM. n.s., not significant. ***$p < 0.001$, ****$p < 0.0001$.

Figure S8

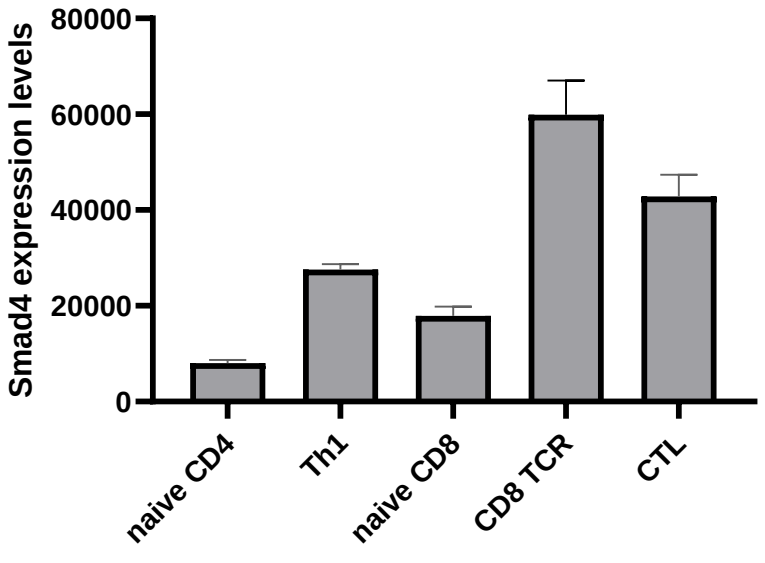

Figure S8 Quantitative analysis of SMAD4 expression levels by mass spectrometry during T cell differentiation. SMAD4 expression levels were significantly elevated in activated $CD4^+$ and $CD8^+$ T cells, compared with naive T cells. Statistical data were collected from this reported study (Howden et al., 2019). CD8 TCR: $CD8^+$ T cells activated *in vitro* for 24 hr; CTL: cytotoxic T cells, $CD8^+$ T cells activated *in vitro* for more than 48 hr.

Figure S9

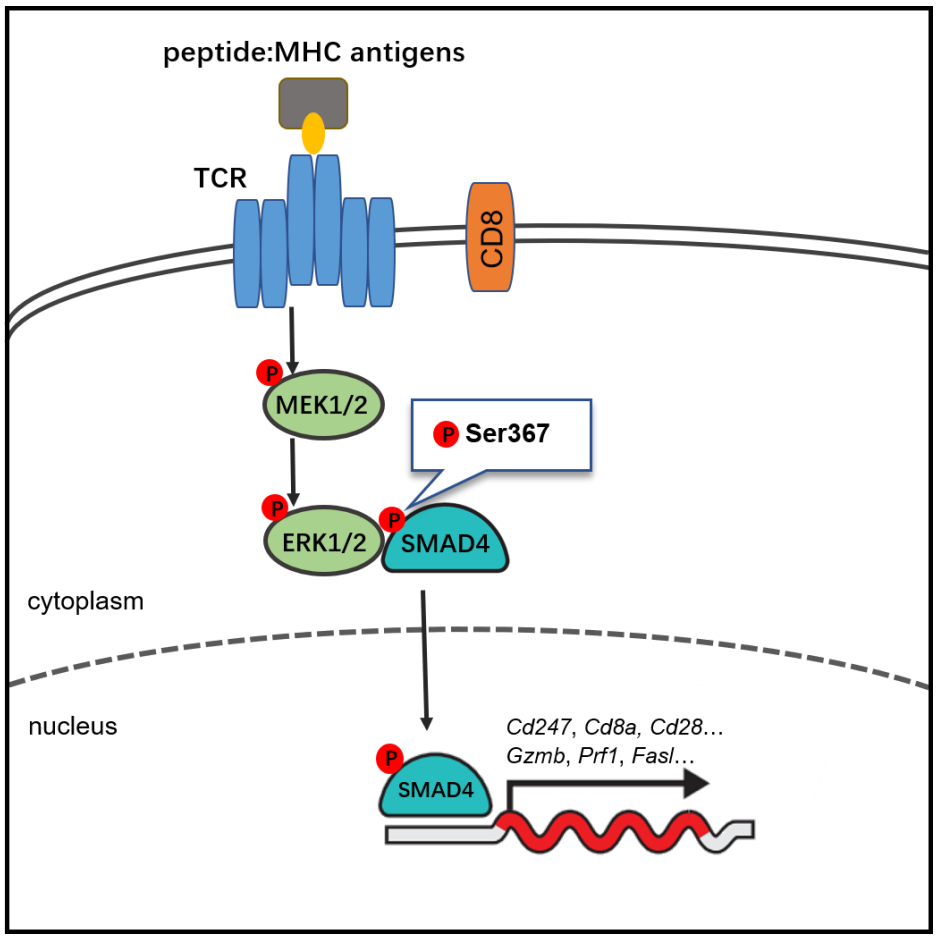

Figure S9 Graphical Abstract. In this study, we found SMAD4 was critical in promoting $CD8^+$ T cell cytotoxic function. SMAD4-mediated transcriptional regulation of $CD8^+$ T cell activation and cytotoxicity is regulated by T-cell receptor (TCR) but not TGF-β signaling pathway. Following TCR activation, SMAD4 was directly phosphorylated by ERK at Ser367 residue and translocated into the nucleus, upregulated genes encoding TCR signaling components and cytotoxic molecules in $CD8^+$ T cells, and thus reinforced T cell function.

Supplemental Excel File 1. RNA-seq results of OVA-specific CD8^{+} TILs from E.G7-bearing wild-type and *Cd8*^{Cre}*Smad4*$^{fl/fl}$ mice

Supplemental Excel File 2. GO and KEGG pathway analysis of SMAD4 down-regulated or up-regulated genes between OVA-specific CD8^{+} TILs from WT and *Cd8*^{Cre}*Smad4*$^{fl/fl}$ mice.

Supplemental Excel File 3. SMAD4 ChIP-seq binding gene loci and KEGG pathway analysis.